

Article

Double-Layer Membranes of Chitosan and Sodium Alginate Added to Natural Olive Leaf Extract for Potential Use in Skin Lesions

Larah Gondim Santos Paulino ¹, Luisa Bataglin Avila ², Caroline Costa Moraes ³ , Mohammad Rizwan Khan ⁴ , Salim Manoharadas ⁵ , Gladson Simões dos Reis ⁶ , Guilherme Luiz Dotto ^{2,*}  and Gabriela Silveira da Rosa ³ 

¹ Chemical Engineering, Federal University of Pampa, Bagé 96413-172, Brazil; larahpaulino.aluno@unipampa.edu.br

² Research Group on Adsorptive and Catalytic Process Engineering (ENGEpac), Federal University of Santa Maria, Santa Maria 97105-900, Brazil; luisabataglinavila@gmail.com

³ Graduate Program in Science and Engineering of Materials, Federal University of Pampa, Bagé 96413-172, Brazil; carolinemoraes@unipampa.edu.br (C.C.M.); gabrielarosa@unipampa.edu.br (G.S.d.R.)

⁴ Department of Chemistry, College of Science, King Saud University, Riyadh 11451, Saudi Arabia; mrkhan@ksu.edu.sa

⁵ Department of Botany and Microbiology, College of Science, King Saud University, Riyadh 11451, Saudi Arabia; smanoharadas@ksu.edu.sa

⁶ Department of Forest Biomaterials and Technology, Biomass Technology Centre, Swedish University of Agricultural Sciences, SE-901 83 Umeå, Sweden; glaydson.simoes.dos.reis@slu.se

* Correspondence: guilherme_dotto@yahoo.com.br



Citation: Paulino, L.G.S.; Avila, L.B.; Moraes, C.C.; Khan, M.R.; Manoharadas, S.; dos Reis, G.S.; Dotto, G.L.; da Rosa, G.S. Double-Layer Membranes of Chitosan and Sodium Alginate Added to Natural Olive Leaf Extract for Potential Use in Skin Lesions. *Resources* **2023**, *12*, 97. <https://doi.org/10.3390/resources12090097>

Academic Editor: Eva Pongrácz

Received: 6 July 2023

Revised: 11 August 2023

Accepted: 17 August 2023

Published: 22 August 2023



Copyright: © 2023 by the authors. Licensee MDPI, Basel, Switzerland. This article is an open access article distributed under the terms and conditions of the Creative Commons Attribution (CC BY) license (<https://creativecommons.org/licenses/by/4.0/>).

Abstract: This study seeks to enhance bilayer membranes using a combination of chitosan and sodium alginate (CS/SA) with phytochemical compounds extracted from olive leaves (CS/SA-OLE), intended for use as a skin dressing. Olive leaf extracts (OLE) were sustainably obtained and showed a phenolic composition of $114.49 \text{ mgGAE}\cdot\text{g}^{-1}$ and antioxidant activity of 94.25%. CS/AS and CS/SA-OLE were prepared using the casting method. The results showed that the addition of OLE improved the mechanical and barrier properties of the membranes. The elongation at break increased from 9.99 to 14.68%, and the water transmission rate reduced from $2207.78 \text{ g}\cdot\text{m}^{-2}\cdot24 \text{ h}^{-1}$ after the addition of OLE. The FTIR spectra showed functional groups of phenolic compounds, and the thermogravimetric analysis showed that the addition of OLE improved the thermal stability of the membranes. In addition, the CS/SA-OLE membranes showed active potential with inhibition halos (12.19 mm) against the microorganism *Escherichia coli*. The membranes generated in this research, particularly those with the addition of natural extracts, exhibit significant promise for utilization as wound dressings.

Keywords: wound dressing; bioactive compounds; biopolymer

1. Introduction

Skin is the outermost body layer, in continuous contact with the environment, and is highly prone to structural damage capable of limiting its protective barrier [1,2]. In general, the healing process involves several complex and dynamic events. However, bacterial colonization and subsequent infections are currently some of the factors responsible for complications in the healing process [2–4]. In this sense, several studies have expanded the possibilities of formulating dressings using biomaterials that favor a biological and effective response in the healing process. In general, membranes obtained from natural polymers have been explored as alternatives for the treatment of skin wounds due to their ability to stimulate the immune system, form granular tissue, promote antimicrobial protection and fibroblast migration, and good selectivity and biocompatibility, besides being natural

biomolecules that reduce environmental pollution [5–7]. Thus, an optimal wound dressing used for physiological skin reconstruction must meet some requirements, such as absorbing excess exudate, keeping the wound moist, and being non-toxic, as well as having barrier properties, high porosity, flexibility, and mechanisms that facilitate treatment and tissue recovery more quickly and efficiently [8–10].

In this context, using two or more combined polymers has shown multiple favorable characteristics for their application as skin dressings due to the possibility of developing biocompatible surfaces without changing the functionality of each material [8,11]. Thus, the combination of sodium alginate and chitosan has been prominent in studies for the development of membranes due to increased mechanical stability, absorption capacity, and a suitable wetting medium for the healing process, in addition to the characteristics present in their structures, such as biocompatibility, biodegradability, barrier properties, non-immunogenicity, and non-toxicity [12–15].

According to studies, using eco-friendly agents in polymeric matrices has promoted the development of bioactive surfaces (antioxidant and antimicrobial) capable of effectively accelerating the recovery of skin integrity. [16]. In addition, applying natural extracts has been encouraged as an alternative to reduce the increasing threat of antibiotic resistance and toxicity [17]. Among the natural sources of bioactive compounds, olive leaves (*Olea europaea* L.) stand out because they are industrial by-products of olive growing, an important activity in the southern region of Rio Grande do Sul, Brazil. In addition, it is known that the olive pruning and harvesting stages generate a large number of olive leaves with a composition rich in phytochemicals, which have been widely used in the formulation of dressings to improve antimicrobial properties due to their effectiveness against Gram-positive (*Staphylococcus aureus*) and Gram-negative bacteria (*Escherichia coli*) [18–21]. The phenolic compounds in olive leaf extract (OLE) composition, such as oleuropein, hydroxytyrosol, and tyrosol, promote antimicrobial activities [22–24]. Furthermore, oleuropein is noteworthy as the main compound responsible for several pharmacological activities, such as hypotensive, antioxidant, hypoglycemic, hypocholesterolemic, antitumor, radio-protective, and anti-inflammatory effects [18,19,22–26], which allow an improvement in biological behavior when applied to dressing materials.

Thus, this work aims to recover the bioactive compounds in olive leaves, proposing their sustainable use as natural actives in chitosan and sodium alginate bilayer membranes for potential application in treating cutaneous wounds. The produced membranes are evaluated according to their thickness, mechanical properties, fluid drainage capacity (FDC), water vapor transmission rate (WVTR), and antimicrobial activity using thermogravimetric analysis (TGA), Fourier transform infrared spectroscopy (ATR-FTIR), and scanning electron microscopy (SEM).

2. Materials and Methods

2.1. Sample Preparation

Olive leaves (*Olea europaea* L., Arbequina) were collected at Estância Guarda Velha, located in Pinheiro Machado, Rio Grande do Sul ($31^{\circ}30'04.0''$ S, $53^{\circ}30'42.0''$ W). After being harvested, the leaves were submitted to a sanitization process. First, the samples were washed in running water; subjected to a commercial solution of sodium hypochlorite, 2% to 2.5% (v/v), for 5 min; and finally, washed with distilled water. Then, they were dried in an oven at 40°C for 24 h, following the methodology proposed by Martiny et al. [27]. The dried samples were ground in an analytical mill (IKA, A11, Darmstadt, Germany), and standardized using a 60-mesh sieve, manufactured to ABNT/ASTM/TYLER standard (Bertel Indústria Metalúrgica Ltda., Caieiras, Brazil), to obtain a particle diameter smaller than 0.272 mm.

2.2. Preparation of the Extracts

Olive leaf extracts (OLE) were obtained using a dynamic maceration process, following the methodology described by Martiny et al. [27]. In this method, 1 g of OLE was added

to 50 mL of distilled water and placed in a Dubnoff metabolic bath (QUIMIS, Diadema, Brazil) for 2 h at 88 °C under constant stirring. After that, the extracts obtained were filtered under vacuum using Whatman 4 filter paper (Fisher Scientific, Hampton, VA, USA), with a diameter of 125 mm, for subsequent characterization and incorporation in the biopolymeric solution. All tests were performed in triplicate.

2.3. Characterization of Olive Leaf Extracts (OLE)

The OLE were characterized for total phenolic compounds (TPC) using the spectrophotometric method described by Singleton and Rossi [28]. The TPC characterization was performed in triplicate, quantified using a gallic acid standard curve, and expressed as milligrams of gallic acid equivalent per gram of dry matter ($\text{mgGAE}\cdot\text{g}^{-1}$ b·s). The OLEs' antioxidant activity (AA) was also evaluated using the method developed by Brand-Williams, Cuvelier, and Berset [29]. Thus, AA evaluation was performed using a 1,1-diphenyl-2-picrylhydrazyl (DPPH) reagent and quantified using Equation (1).

$$\text{AA}(\%) = \frac{A_b - A_a}{A_b} 100 \quad (1)$$

where AA (%) is the antioxidant activity, A_b is the absorbance of the blank, and A_a is the absorbance of the OLE.

2.4. Synthesis of the Bilayer Membranes

The bilayer membranes CS/SA and CS/SA-OLE were obtained by adapting the methodology described by Wang et al. [11], and Figure 1 summarizes the process.

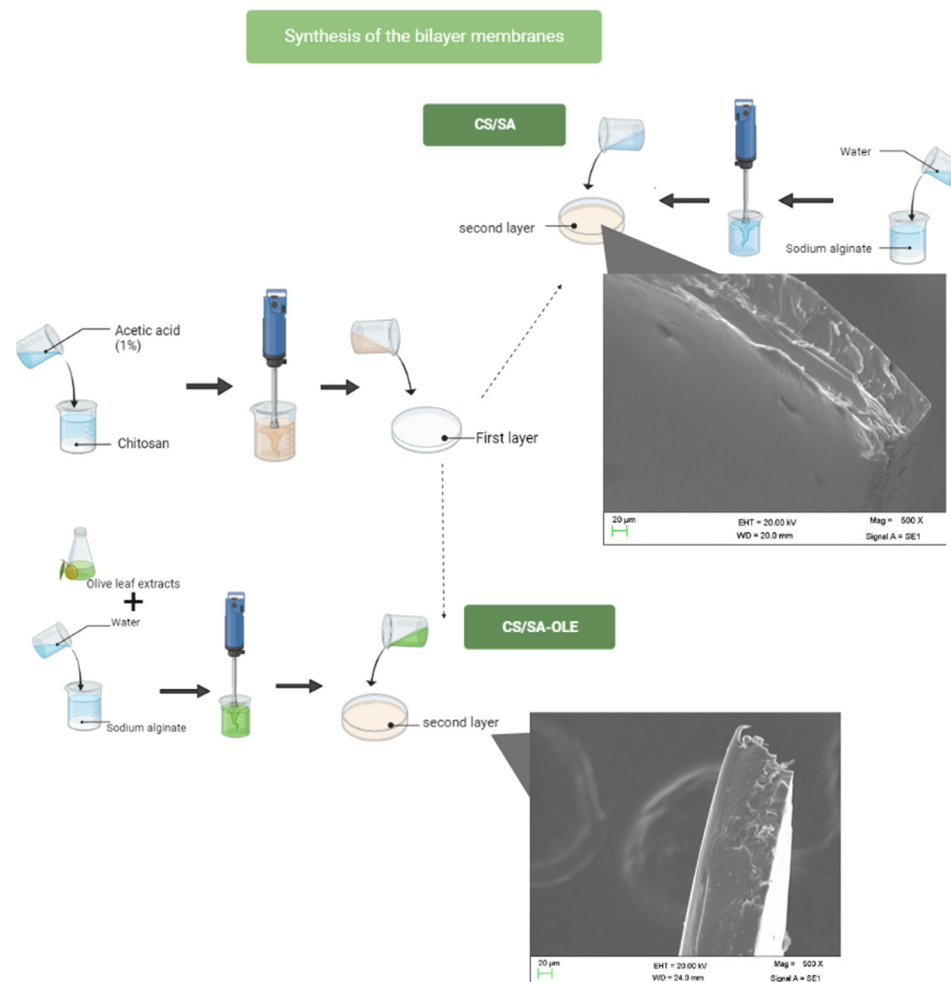


Figure 1. Scheme for obtaining CS/SA and CS/SA-OLE membranes.

The first layer was composed of chitosan (CS) (molecular weight of 150 kDa, deacetylation degree of 85%, and particle size of 72 μm) and produced using the polymer ratio of 1:100 (*m/v*) with acetic acid 1% (*v/v*) as the solvent. The solutions were rested for 24 h and then subjected to constant stirring (193 rpm) for 15 min until a homogeneous mixture was formed. They were then dried in an oven at 40 °C for 7 h until a consistent surface was formed. The second layer was obtained by adding sodium alginate (AS) in a 1:100 (*m/v*) ratio in distilled water at room temperature. The solutions were subjected to constant stirring (193 rpm) for 1 h until a homogeneous mixture was formed. They were then poured over the first layer and taken to the oven for 12 h to obtain the CS/SA membranes.

The bilayer membranes (CS/SA-OLE) were obtained using the same methodology; however, part of the water that was used to solubilize the sodium alginate was substituted with the liquid extract. Thus, sodium alginate solutions (second layer of the membrane) were prepared by dissolving the polymer in 75 mL of aqueous olive leaf extract and 25 mL of distilled water.

2.5. Characterization of Membranes

The thickness of the membranes was determined using a digital micrometer (Insize-IP65, São Paulo, Brazil) at ten random positions over the area of the membranes.

The mechanical properties, tensile strength, and elongation at break of the membranes were evaluated using a texturometer (STABLE MICRO SYSTEM—TA.XT.plus, Surrey, UK) with a 50 N load cell, following the standard [30]. The distance of the grips was 50 mm with a speed of 50 $\text{mm}\cdot\text{min}^{-1}$. The analyses were performed in triplicate at room temperature and determined using Equations (2) and (3):

$$T = \frac{F_m}{A_{min}} \quad (2)$$

$$E(\%) = \frac{d_r}{d_i} 100 \quad (3)$$

where T represents the tensile strength (MPa), F_m is the maximum force measured at membrane rupture (N), A_{min} is the minimum cross-sectional area of the membrane (m^2), E (%) is the elongation at break, d_r is the distance at rupture traveled by the movable grips (cm), and d_i is the initial distance between the grips (cm).

Fluid drainage capacity (FDC) and water vapor transmission rate (WVTR) analyses were carried out following the BS EN 13726-1 method [31], where the membranes (CS/SA and CS/SA-OLE) were cut into disks of a 2.7 cm diameter and weighed and attached to the ends of modified Paddington cups containing 20 mL of simulated body fluid (SBF). The tubes were weighed and inverted so that the samples came in contact with the SBF. The samples were then incubated in an oven in desiccators containing silica gel for 24 h at 37 °C. The water vapor transmission rate (WVTR) and fluid drainage capacity (FDC) were determined using Equations (4) and (5), respectively.

$$\text{WVTR} = \frac{m_{is} - m_{fs}}{tA} \quad (4)$$

$$\text{FDC} = \frac{m_{is} - m_{fs}}{tA} - \frac{m_{im} - m_{fm}}{tA} \quad (5)$$

where m_{is} is the initial mass of the system, m_{fs} is the final mass of the system after the drainage period, m_{im} is the initial mass of the membrane, m_{fm} is the final mass of the membrane after the drainage period, A is the contact area between the membrane and the fluid, and t is the time.

The thermal stability of the membranes was evaluated through thermogravimetric analysis (TGA) using a thermogravimetric instrument (SHIMADZU TGA 50, Kyoto, Japan). For this assay, approximately 5 mg of the membrane samples were heated in platinum

capsules over a range from 30 °C to 900 °C and at a heating rate of 10 °C·min⁻¹ with a nitrogen flow rate of 50 mL·min⁻¹.

The functional groups in the bilayer membranes were investigated using the Fourier transform infrared spectroscopy (ATR-FTIR) technique (SHIMADZU, Prestige 21, Nakagyo-ku, Kyoto, Japan) in a range from 400 cm⁻¹ to 4000 cm⁻¹ and a resolution of 4 cm⁻¹.

The membranes were evaluated for morphology by applying gold films to the previously prepared samples and were analyzed using scanning electron microscopy (SEM) at 500 and 1000× magnifications (EVO MA10, Carl Zeiss, Jena, Germany).

2.6. Antimicrobial Activity

The bilayer membranes, with and without OLE, were studied for their microbial inhibition potential using the disk diffusion method [32]. The test was performed using an inoculated Tryptic Soy Agar (TSA) medium, where microorganisms were prepared in nutrient broths and incubated at 35 °C for 24 h. The sterilized agar plates were inoculated evenly with 10⁵ CFU/cm² of the microorganisms *Escherichia coli* (Gram-negative, ATCC 11229) and *Staphylococcus aureus* (Gram-positive, ATCC 12598). After that, the samples, which were cut into disks (7.5 mm) and previously sterilized under ultraviolet light (15 min for each side of the bilayer sample), were placed in contact with the contaminated Mueller-Hinton agar, and the plates were incubated at 37 °C for 24 h. After the incubation, the zone of inhibition (inhibition halos) formed by the samples for each microorganism tested was determined.

2.7. Statistical Analysis

The results were presented as mean ± standard deviation and statistically analyzed using a *t*-test with a 95% significance level using the STATISTICA Ultimate Academic software, version 10.0 (Starsoft Inc., Naperville, IL, USA).

3. Results and Discussion

3.1. Characteristics of Bioactive Compounds from Olive Leaves

The results obtained from the total phenolic compounds (TPC) and antioxidant activity (AA) analyses were 114.49 mgGAE·g⁻¹ (b·s) and 94.25%, respectively. Lamprou et al. [33] obtained a TPC content of 86.4 mgGAE·g⁻¹ for the OLE, Koroneiki variety extract, using water and 6.4% sulfuric acid (*w/w*) as the extracting solvent. Martiny et al. [21], using dynamic maceration and water as the extracting solvent, obtained a TPC content of 115.96 mgGAE·g⁻¹, and Valério Filho et al. [18] obtained a TPC content of 41.64 mgGAE·g⁻¹ for the OLE, cultivar Arbequina, using water as the extracting solvent. As for AA, the results found in this study (94.25%) were close to those reported in the literature by Moudache et al. [34], who, after 2 h of extraction, obtained an AA concentration of 95.4% for olive leaf extract. Filho et al. [18] obtained an AA concentration of 95.23% using the solid-liquid maceration method. Rosa et al. [24] obtained an AA concentration of 90.03% for the OLE using water as the solvent and the microwave-assisted extraction method. The results of the TPC and AA analyses found in the present work were similar to those obtained by the cited authors. The differences in TPC concentration and AA may be related to the cultivar variation. According to studies presented in the literature, the geographical and climatic origins of the cultivar can significantly influence the concentration of bioactive compounds present in olive leaves, with climatic conditions near the Mediterranean being the most favorable for the highest concentration of polyphenols [35]. In addition, other factors influence the process yield, such as the extraction technique and extraction solvent [36]. Given the results of the characterization of the OLE, the high presence of oleuropein demonstrates a potential application in skin dressings due to its healing properties [37].

3.2. Characteristics of Bilayer Membranes

The CS/SA and CS/SA-OLE membranes were characterized concerning their thickness, tensile strength, elongation at break, fluid drainage capacity, and water transmission rate, and the results are presented in Table 1.

Table 1. Characterization of membranes.

	CS/AS	CS/SA-OLE
Thickness (mm)	0.14 ± 0.02 ^a	0.22 ± 0.01 ^b
Tensile Strength (MPa)	4.214 ± 0.905 ^a	2.994 ± 0.239 ^b
Elongation at break (%)	9.990 ± 3.011 ^a	14.686 ± 1.700 ^a
Fluid drainage capacity (g·m ⁻² ·24 h ⁻¹)	1959.929 ± 7.517 ^a	2083.470 ± 13.559 ^b
Water transmission rate (g·m ⁻² ·24 h ⁻¹)	2207.28 ± 4.54 ^a	2094.33 ± 17.08 ^b

Data reported are mean values ± standard deviation ($n = 3$). (a,b) Different letters in the same line represent significant differences among the samples ($p < 0.05$) using the *t*-test.

According to Table 1, the results obtained for the thickness were 0.14 mm for the CS/SA and 0.22 mm for the CS/SA-OLE membranes. It was found that the addition of OLE caused a significant increase in this value. This observed effect occurred due to the linear increase in mass of the film-forming solution with the addition of the extract [19]. This effect was also reported by Arieta et al. [36], who obtained thicknesses of 0.055 mm and 0.063 mm for low-density polyethylene and cellulose acetate bilayer membranes without and with *Cucumis metuliferus* extract, respectively. Avila et al. [38] obtained a thickness of 0.50 mm for chitosan and zein bilayer films with 3% jaboticaba (*Plinia cauliflora*) peel extract. Da Rosa et al. [39] also reported an increase in the thickness of films with different concentrations of olive leaf extract. The thickness values reported in this work are close to those described in the literature and smaller than the human dermis, which ranges between 0.5 and 2.0 mm depending on factors such as age, sex, and body part [40], and this is a desirable characteristic for the applicability of a skin patch.

The CS/SA membranes exhibited a tensile strength of 4.214 MPa and an elongation at a break of 9.990%. However, the tensile strength of the bilayer membranes decreased after incorporating the OLE. In the present work, the CS/SA-EFO bilayer membranes exhibited a slightly higher elongation at break (14.686%) compared to the CS/SA membranes, although without significant differences, probably due to the presence of lipid components that acted as plasticizers in the active membranes [19]. Mouro et al. [17] evaluated the mechanical properties of polycaprolactone, poly(vinyl alcohol), and chitosan-tripolyphosphate membranes with and without *Centella asiatica* (L.) extract and reported a reduction in the tension and elongation of the membranes from 3.96 MPa to 3.03 MPa and 10.39% to 8.31%, respectively. In general, the parameters for applying the skin dressing will depend on the body region where the material will be inserted. Thus, the values obtained in the present study were close to those exhibited by human skin, which presents elongation between 10% and 115% and tensile strength between 2.5 and 30 MPa [41], demonstrating that the material can provide less damaging mechanical conditions at the lesion site [42,43].

The FDC values found in the present study were 1959.93 g·m⁻²·h⁻¹ and 2083.47 g·m⁻²·24 h⁻¹ for the membranes without (CS/SA) and with (CS/SA-OLE) the addition of the extract, respectively. The addition of OLE resulted in a high FDC; this increase may be associated with the oleuropein present in the extract, which improved the hydrophilic properties of the membranes. Geneviro [44] obtained a maximum permeation of 3530.8 g·m⁻²·24 h⁻¹ in konjac glucomannan membranes. Analyzing the results obtained in the literature, it was possible to observe that the permeation values presented in this study would not support the high volume of exudates (between 3400 and 5100 g·m⁻²·24 h⁻¹) generated during the healing process of injuries such as third-degree burns [45]. However, the FDC results are applicable for less severe injuries such as first-degree burns,

($278.4 \text{ g} \cdot \text{m}^{-2} \cdot 24 \text{ h}^{-1}$) [42–44]. The moisture in the wound region must be controlled to achieve optimal healing rates. Thus, the FDC is an important factor in developing skin dressings, as it is a parameter capable of preventing the accumulation of exudates and excessive dehydration of the lesion [41].

The water vapor transmission rate (WVTR) is a parameter for monitoring the ideal oxygenation capacity of a skin dressing for the healing process to occur, and according to studies, the range should be between 2000 and $2500 \text{ g} \cdot \text{m}^{-2} \cdot 24 \text{ h}^{-1}$ [17,46]. In this sense, the values obtained in the present study (2207.28 and $2094.33 \text{ g} \cdot \text{m}^{-2} \cdot 24 \text{ h}^{-1}$ for CS/SA and CS/SA-OLE, respectively) are within the ideal oxygenation range for application in skin dressings. Surendranath et al. [47] developed a zein/PEO membrane for wound healing and obtained a WVTR in the range of 1500 – $2000 \text{ g} \cdot \text{m}^{-2} \cdot 24 \text{ h}^{-1}$. Mouro et al. [17] developed bilayer membranes with and without natural extract (*Centella asiatica* L.) and analyzed the WVTR of the material, obtaining rates of $1162.94 \text{ g} \cdot \text{m}^{-2} \cdot 24 \text{ h}^{-1}$ and $1757.12 \text{ g} \cdot \text{m}^{-2} \cdot 24 \text{ h}^{-1}$ for the membranes with and without extract, respectively. According to Garcia-Orue et al. [48], the WVTR of commercial dressings is between 426 and $2047 \text{ g} \cdot \text{m}^{-2} \cdot 24 \text{ h}^{-1}$. Thus, the membranes tested in this study have the potential for application as dressings, as they are within the applicability range of commercial dressings.

The TGA and differential thermal analysis (DTA) curves of the bilayer membranes with (green line) and without (red line) OLE are shown in Figure 2.

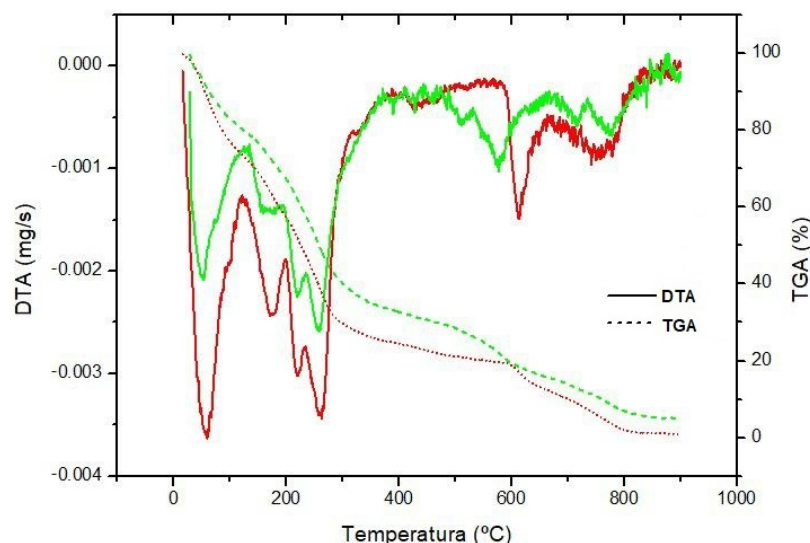


Figure 2. Thermogravimetric curves of the bilayer membranes without and with the addition of olive leaf extract.

The thermogravimetric analysis (TGA) curves show that the CS/SA membranes decomposed similarly to the CS/SA-OLE membranes. Based on the results, a constant weight loss was observed in the temperature range of 80 – $800 \text{ }^{\circ}\text{C}$. Thus, the mass loss peaks between 100 and $190 \text{ }^{\circ}\text{C}$ can be attributed to the evaporation of water, volatile components, and glycerol [49,50]. The peak at $220 \text{ }^{\circ}\text{C}$ (third peak) can be related to the degradation of the sodium alginate polymer chains [51]. Zhang et al. [52] reported sodium alginate degradation at $235 \text{ }^{\circ}\text{C}$ and $246 \text{ }^{\circ}\text{C}$, respectively. The fourth peak of mass loss was observed between 250 and $300 \text{ }^{\circ}\text{C}$, which was related to the dehydration of saccharide rings, depolymerization, and the decomposition of acetylated units of the chitosan [53]. The degradation rate of both materials decreased after $400 \text{ }^{\circ}\text{C}$. The fifth mass loss peak of the membranes (CS/SA and CS/SA-OLE) was found near $580 \text{ }^{\circ}\text{C}$ and $600 \text{ }^{\circ}\text{C}$, which represents the residual mass values from the incomplete degradation of the inorganic compounds present in each polymer and the degradation rate of olive leaf extract [54]. Erdogan, Demir, and Bayraktar [55] observed non-degraded mass at $600 \text{ }^{\circ}\text{C}$, estimating that degradation would be complete at temperatures above $800 \text{ }^{\circ}\text{C}$. The CS/SA membranes

were fully degraded after 800 °C, whereas the CS/SA-OLE membranes showed that 5% to 10% of their mass was not degraded [55].

The ATR-FTIR analysis of the membranes without extract (CS/SA) and with extract (CS/SA-OLE) is presented in Figure 3.

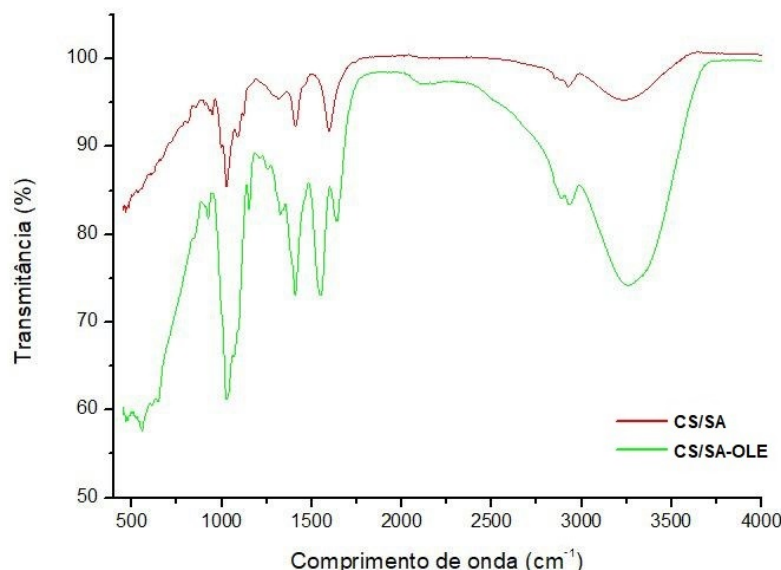


Figure 3. ATR-FTIR analysis of the chitosan and sodium alginate bilayer membranes, both pure (CS/SA) and with olive leaf extract (CS/SA-OLE).

The ATR-FTIR spectra studied showed bands between 3000 and 3500 cm⁻¹ in both materials (CS/SA and CS/SA-OLE), which were related to the O-H stretching vibrations of the hydroxyl groups present in polysaccharides, such as chitosan and sodium alginate, as well as water [56,57]. In addition, a broadening of this peak was observed for the CS/SA-OLE samples compared to the CS/SA samples, possibly due to compounds present in the extract, such as oleuropein [35]. The bands around 2800 and 3000 cm⁻¹ were assigned to C-H stretching [58], being more pronounced in the CS/SA-OLE membrane spectrum due to the additional groups in the extract. Other vibration bands characteristic of polymers were observed in the CS/SA and CS/SA-OLE spectra, such as the carboxylate group, with an asymmetric stretch observed at 1600 cm⁻¹ and a symmetric stretch at around 1420 cm⁻¹, as well as a C-O stretch vibration represented at 1030 cm⁻¹ [9]. The peaks observed in the present study are similar to those found by other authors in chitosan and sodium alginate-based materials [8,9,56]. In addition, the peaks obtained from the CS/SA showed a negligible shift between them, which can be explained by the electrostatic interactions between the various functional groups present in the chitosan and sodium alginate membranes, mainly through hydrogen bonds, which caused the overlapping of the spectra [59,60].

The SEM images of the CS/SA and CS/SA-OLE membranes are shown in Figure 4. In the SEM images of the membrane surface, both samples showed homogeneous surfaces. The images showed a compact structure without separation of the layers, and the good adhesion of the polymers to the membranes with the extract (CS/SA-OLE) was more visible, suggesting that the morphology of each material was preserved.

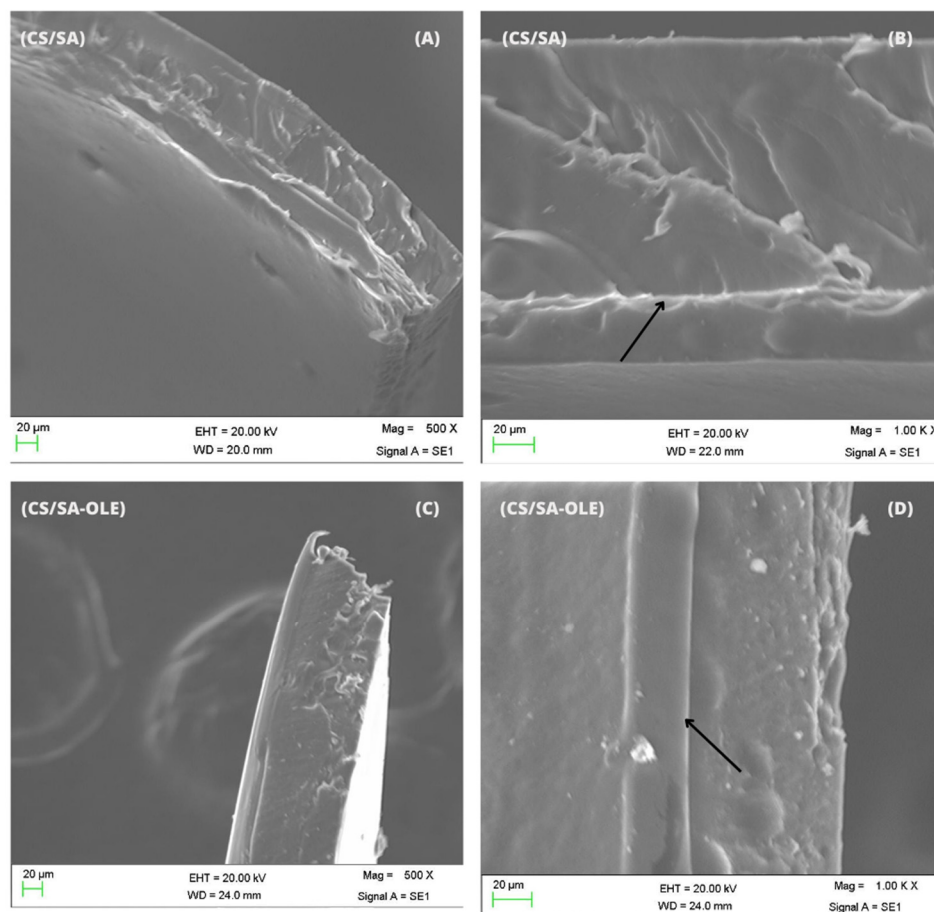


Figure 4. SEM images of the cross-sections of the CS/SA and CS/SA-OLE bilayer membranes: (A,B) at 500 \times ; (C,D) at 1000 \times .

3.3. Antimicrobial Potential of Bilayer Membranes

Figure 5 illustrates the analysis of the microbial potential of the bilayer membranes against *Escherichia coli* (*E. coli*) and *Staphylococcus aureus* (*S. aureus*). Table 2 presents the values for the inhibition halos.

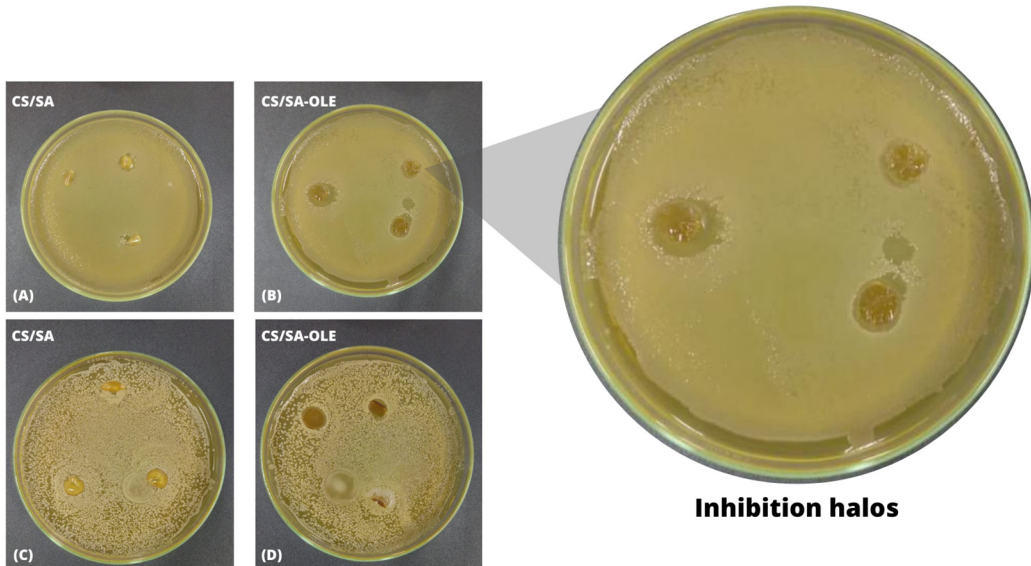


Figure 5. Microbial analysis against strains: (A,B) *E. coli*; (C,D) *S. aureus*.

Table 2. Diameters of the inhibition zone.

	<i>Staphylococcus aureus</i>	<i>Escherichia coli</i>
CS/SA (mm)	0.0	0.0
CS/SA-OLE (mm)	0.0	12.19 ± 0.98

Table 2 shows that CS/SA-OLE showed inhibition halos against the microorganism *E. coli*, indicating the presence of antimicrobial activity in the membranes with the natural extract. However, the pure membranes (CS/SA) did not show an inhibition zone for either of the two strains studied (*Escherichia coli* and *Staphylococcus aureus*). Bayraktar [61] also observed the absence of inhibition in his silk fibroin nanofibers without olive leaf extract for the studied species (*Staphylococcus epidermidis* and *Escherichia coli*) in his work. Similarly, Avila et al. [38] verified inhibition halos of 8.77 ± 0.31 mm for *E. coli* and 9.32 ± 0.21 mm for *S. aureus* in chitosan and zein fiber bilayer films with added jaboticaba peel extract, whereas the films without extract showed no inhibition against the microorganisms evaluated. Luciano et al. [62] developed bilayer gelatin films incorporated with pitanga leaf hydroethanolic extract and obtained an inhibition zone of 6.9 mm against the *S. aureus* microorganism.

The inhibition ability of CS/SA-OLE can be attributed to the high concentration of polyphenols, with an emphasis on oleuropein, present in the OLE obtained in this study [63]. Thus, the inhibition tests showed the potential application of CS/SA-OLE membranes as skin dressings.

4. Conclusions

The research findings revealed an abundance of total polyphenols and high antioxidant activity within the olive leaf extracts (OLE), indicating a potential source of bioactive compounds. These results reinforce the potential for recovering bioactive compounds from agricultural waste for use as a natural additive. This approach offers advantages such as cost-effectiveness due to being a by-product of olive cultivation. The characterization of chitosan and sodium alginate bilayer membranes showed good flexibility, ease of manipulation, and excellent adhesion between the layers. The inclusion of OLE significantly improved the material properties, such as the fluid drainage capacity and water vapor transmission rate. The addition of OLE reduced the tensile strength and resulted in a slight change in elongation at the break of the material. The membranes enriched with OLE exhibited remarkable features, including inhibition zones against the *E. coli* microorganism. Therefore, this study presented encouraging results for applying membranes as cutaneous dressings. However, further comprehensive studies, including *in vivo* testing, are required to validate this potential.

Author Contributions: Conceptualization, L.G.S.P. and L.B.A.; methodology, L.G.S.P. and L.B.A.; formal analysis, L.G.S.P.; investigation, L.G.S.P.; resources, L.G.S.P.; data curation, L.G.S.P.; writing—original draft preparation, L.G.S.P., L.B.A., C.C.M., G.L.D. and G.S.d.R. (Glaydson Simões dos Reis); writing—review and editing, L.G.S.P., L.B.A., C.C.M., G.L.D. and G.S.d.R. (Glaydson Simões dos Reis); visualization, L.G.S.P., L.B.A., S.M., G.S.d.R. (Gabriela Silveira da Rosa), C.C.M., M.R.K., G.L.D. and G.S.d.R. (Gabriela Silveira da Rosa); supervision, G.S.d.R. (Gabriela Silveira da Rosa). All authors have read and agreed to the published version of the manuscript.

Funding: This research was funded by the Coordination for the Improvement of Higher Education Personnel (CAPES) (PGCI88887.125421/2016-001), the Research Support Foundation of the State of Rio Grande do Sul (FAPERGS), the National Council for Scientific and Technological Development (CNPq), the Federal University of Pampa (UNIPAMPA), and the Federal University of Santa Maria (UFSM).

Institutional Review Board Statement: Not applicable.

Data Availability Statement: Not applicable.

Acknowledgments: The authors thank the Research Support Foundation of the State of Rio Grande do Sul (FAPERGS), the Federal University of Pampa and National Council for Scientific and Technological Development (CNPq). The authors thank the Research Supporting Project for funding this work through the Research Supporting Project number (RSPD2023R708), King Saud University, Riyadh, Saudi Arabia. dos Reis thanks Bio4Energy—a Strategic Research Environment appointed by the Swedish government and the Swedish University of Agricultural Sciences—for the funding support.

Conflicts of Interest: The authors declare no conflict of interest.

References

1. Tamer, T.M.; Sabet, M.M.; Omer, A.M.; Abbas, E.; Eid, A.I.; Mohy-Eldin, M.S.; Hassan, M.A. Hemostatic and antibacterial PVA/Kaolin composite sponges loaded with penicillin–streptomycin for wound dressing applications. *Sci. Rep.* **2021**, *11*, 3428. [[CrossRef](#)]
2. Xue, M.; Zhao, R.; Lin, H.; Jackson, C. Delivery systems of current biologicals for the treatment of chronic cutaneous wounds and severe burns. *Adv. Drug Deliv. Rev.* **2018**, *129*, 219–241. [[CrossRef](#)]
3. Alminderej, F.M. Study of new cellulosic dressing with enhanced antibacterial performance grafted with a biopolymer of chitosan and myrrh polysaccharide extract. *Arab. J. Chem.* **2020**, *13*, 3672–3681. [[CrossRef](#)]
4. Yin, J.; Xu, L. Batch preparation of electrospun polycaprolactone/chitosan/aloe vera blended nanofiber membranes for novel wound dressing. *Int. J. Biol. Macromol.* **2020**, *160*, 352–363. [[CrossRef](#)]
5. Hassan, M.A.; Tamer, T.M.; Valachová, K.; Omer, A.M.; El-Shafeey, M.; Mohy Eldin, M.S.; Šoltés, L. Antioxidant and antibacterial polyelectrolyte wound dressing based on chitosan/hyaluronan/phosphatidylcholine dihydroquercetin. *Int. J. Biol. Macromol.* **2021**, *166*, 18–31. [[CrossRef](#)]
6. Zhao, X.; Guo, B.; Wu, H.; Liang, Y.; Ma, P.X. Injectable antibacterial conductive nanocomposite cryogels with rapid shape recovery for noncompressible hemorrhage and wound healing. *Nat. Commun.* **2018**, *9*, 2784. [[CrossRef](#)]
7. Fang, H.; Wang, J.; Li, L.; Xu, L.; Wu, Y.; Wang, Y.; Fei, X.; Tian, J.; Li, Y. A novel high-strength poly(ionic liquid)/PVA hydrogel dressing for antibacterial applications. *Chem. Eng. J.* **2019**, *365*, 153–164. [[CrossRef](#)]
8. de Espíndola Sobczyk, A.; Luchese, C.L.; Faccin, D.J.L.; Tessaro, I.C. Influence of replacing oregano essential oil by ground oregano leaves on chitosan/alginate-based dressings properties. *Int. J. Biol. Macromol.* **2021**, *181*, 51–59. [[CrossRef](#)] [[PubMed](#)]
9. Zhu, J.; Wu, H.; Sun, Q. Preparation of crosslinked active bilayer film based on chitosan and alginate for regulating ascorbate–glutathione cycle of postharvest cherry tomato (*Lycopersicon esculentum*). *Int. J. Biol. Macromol.* **2019**, *130*, 584–594. [[CrossRef](#)] [[PubMed](#)]
10. Kamel, N.A.; Abd El-messieh, S.L.; Saleh, N.M. Chitosan/banana peel powder nanocomposites for wound dressing application: Preparation and characterization. *Mater. Sci. Eng. C* **2017**, *72*, 543–550. [[CrossRef](#)]
11. Wang, L.; Wang, W.; Liao, J.; Wang, F.; Jiang, J.; Cao, C.; Li, S. Novel bilayer wound dressing composed of SIS membrane with SIS cryogel enhanced wound healing process. *Mater. Sci. Eng. C* **2018**, *85*, 162–169. [[CrossRef](#)]
12. Varaprasad, K.; Jayaramudu, T.; Kanikireddy, V.; Toro, C.; Sadiku, E.R. Alginate-based composite materials for wound dressing application: A mini review. *Carbohydr. Polym.* **2020**, *236*, 116025. [[CrossRef](#)]
13. Alavi, M.; Nokhodchi, A. An overview on antimicrobial and wound healing properties of ZnO nanobiofilms, hydrogels, and bionanocomposites based on cellulose, chitosan, and alginate polymers. *Carbohydr. Polym.* **2020**, *217*, 115349. [[CrossRef](#)] [[PubMed](#)]
14. Zhang, M.; Qiao, X.; Han, W.; Jiang, T.; Liu, F.; Zhao, X. Alginate-chitosan oligosaccharide-ZnO composite hydrogel for accelerating wound healing. *Carbohydr. Polym.* **2021**, *266*, 118100. [[CrossRef](#)] [[PubMed](#)]
15. Panawes, S.; Ekabutr, P.; Niamlang, P.; Pavasant, P.; Chuysinuan, P.; Supaphol, P. Antimicrobial mangosteen extract infused alginate-coated gauze wound dressing. *J. Drug Deliv. Sci. Technol.* **2017**, *41*, 182–190. [[CrossRef](#)]
16. Abbas, M.; Arshad, M.; Rafique, M.K.; Altalhi, A.A.; Saleh, D.I.; Ayub, M.A.; Sharif, S.; Riaz, M.; Alshawwa, S.Z.; Masood, N.; et al. Chitosan-polyvinyl alcohol membranes with improved antibacterial properties contained Calotropis procera extract as a robust wound healing agent. *Arab. J. Chem.* **2022**, *15*, 103766. [[CrossRef](#)]
17. Mouro, C.; Fangueiro, R.; Gouveia, I.C. Preparation and Characterization of Electrospun Double-layered Nanocomposites Membranes as a Carrier for *Centella asiatica* (L.). *Polymers* **2020**, *12*, 2653. [[CrossRef](#)] [[PubMed](#)]
18. Valério Filho, A.; Avila, L.B.; Lacorte, D.H.; Martiny, T.R.; Rosseto, V.; Moraes, C.C.; Dotto, G.L.; Carreno, N.L.V.; da Rosa, G.S. Brazilian Agroindustrial Wastes as a Potential Resource of Bioactive Compounds and Their Antimicrobial and Antioxidant Activities. *Molecules* **2022**, *27*, 6876. [[CrossRef](#)]
19. Medina, E.; Romero, C.; García, P.; Brenes, M. Characterization of bioactive compounds in commercial olive leaf extracts, and olive leaves and their infusions. *Food Funct.* **2019**, *10*, 4716–4724. [[CrossRef](#)]
20. Kiritsakis, K.; Goula, A.M.; Adamopoulos, K.G.; Gerasopoulos, D. Valorization of Olive Leaves: Spray Drying of Olive Leaf Extract. *Waste Biomass Valorization* **2018**, *9*, 619–633. [[CrossRef](#)]
21. Şahin, S.; Bilgin, M. Olive tree (*Olea europaea* L.) leaf as a waste by-product of table olive and olive oil industry: A review. *J. Sci. Food Agric.* **2018**, *98*, 1271–1279. [[CrossRef](#)] [[PubMed](#)]
22. Martiny, T.R.; Raghavan, V.; Moraes, C.C.d.; Rosa, G.S.d.; Dotto, G.L. Bio-Based Active Packaging: Carrageenan Film with Olive Leaf Extract for Lamb Meat Preservation. *Foods* **2020**, *9*, 1759. [[CrossRef](#)] [[PubMed](#)]

23. Yahfoufi, N.; Alsadi, N.; Jambi, M.; Matar, C. The Immunomodulatory and Anti-Inflammatory Role of Polyphenols. *Nutrients* **2018**, *10*, 1618. [CrossRef] [PubMed]
24. da Rosa, G.S.; Vanga, S.K.; Gariepy, Y.; Raghavan, V. Comparison of microwave, ultrasonic and conventional techniques for extraction of bioactive compounds from olive leaves (*Olea europaea* L.). *Innov. Food Sci. Emerg. Technol.* **2019**, *58*, 102234. [CrossRef]
25. Ashkanani, M.; Farhadi, B.; Ghanbarzadeh, E.; Akbari, H. Study on the protective effect of hydroalcoholic Olive Leaf extract (oleuropein) on the testis and sperm parameters in adult male NMRI mice exposed to Mancozeb. *Gene Rep.* **2020**, *21*, 100870. [CrossRef]
26. Alcaide-Hidalgo, J.M.; Margalef, M.; Bravo, F.I.; Muguerza, B.; López-Huertas, E. Virgin olive oil (unfiltered) extract contains peptides and possesses ACE inhibitory and antihypertensive activity*. *Clin. Nutr.* **2020**, *39*, 1242–1249. [CrossRef] [PubMed]
27. Martiny, T.R.; Raghavan, V.; de Moraes, C.C.; da Rosa, G.S.; Dotto, G.L. Optimization of green extraction for the recovery of bioactive compounds from Brazilian olive crops and evaluation of its potential as a natural preservative. *J. Environ. Chem. Eng.* **2021**, *9*, 105130. [CrossRef]
28. Singleton, V.L.; Rossi, J.A. Colorimetry of total phenolics with phosphomolybdic-phosphotungstic acid reagents. *Am. J. Enol. Vitic.* **1965**, *16*, 144–158. [CrossRef]
29. Brand-Williams, W.; Cuvelier, M.E.; Berset, C. Use of a free radical method to evaluate antioxidant activity. *LWT-Food Sci. Technol.* **1995**, *28*, 25–30. [CrossRef]
30. ASTM D882-12; Standard Test Method for Tensile Properties of Thin Plastic Sheeting. American Society for Testing and Materials: West Conshohocken, PA, USA, 2012.
31. BS EN 13726-1:2002; Test Methods for Primary Wound Dressings. Part 1: Aspects of Absorbency, Section 3.3 Fluid Handling Capacity. British Standards Institute—BSI: London, UK, 2002.
32. M02A11; Clinical and Laboratory Standards Institute Performance Standards for Antimicrobial Disk Susceptibility Tests. Clinical and Laboratory Standards Institute: Wayne, PA, USA, 2012.
33. Lamprou, G.K.; Vlysidis, A.; Tzathas, K.; Vlyssides, A.G. Statistical optimization and kinetic analysis of the extraction of phenolic compounds from olive leaves. *J. Chem. Technol. Biotechnol.* **2019**, *95*, 457–465. [CrossRef]
34. Moudache, M.; Colon, M.; Nerín, C.; Zaidi, F. Phenolic content and antioxidant activity of olive by-products and antioxidant film containing olive leaf extract. *Food Chem.* **2016**, *212*, 521–527. [CrossRef] [PubMed]
35. Martiny, T.R.; Pacheco, B.S.; Pereira, C.M.P.; Mansilla, A.; Astorga-España, M.S.; Dotto, G.L.; Moraes, C.C.; Rosa, G.S. A Novel Biodegradable Film Based on κ-Carrageenan Activated with Olive Leaves Extract. *Food Sci. Nutr.* **2020**, *8*, 3147–3156. [CrossRef] [PubMed]
36. Arrieta, M.P.; Garrido, L.; Faba, S.; Guarda, A.; Galotto, M.J.; López de Dicastillo, C. Cucumis metuliferus Fruit Extract Loaded Acetate Cellulose Coatings for Antioxidant Active Packaging. *Polymers* **2020**, *12*, 1248. [CrossRef] [PubMed]
37. Samancıoğlu, S.; Esen, A.; Ercan, G.; Mansoub, N.H.; Vatansever, S.; İnce, İ. A new dressing material in diabetic wounds: Wound healing activity of oleuropein-rich olive leaf extract in diabetic rats. *Gaziantep Med. J.* **2016**, *1*, 14–21. [CrossRef]
38. Avila, L.B.; Pinto, D.; Silva, L.F.O.; de Farias, B.S.; Moraes, C.C.; Da Rosa, G.S.; Dotto, G.L. Antimicrobial Bilayer Film Based on Chitosan/Electrospun Zein Fiber Loaded with Jaboticaba Peel Extract for Food Packaging Applications. *Polymers* **2022**, *14*, 5457. [CrossRef] [PubMed]
39. Da Rosa, G.S.; Vanga, S.K.; Gariepy, Y.; Raghavan, V. Development of Biodegradable Films with Improved Antioxidant Properties Based on the Addition of Carrageenan Containing Olive Leaf Extract for Food Packaging Applications. *J. Polym. Environ.* **2020**, *28*, 123–130. [CrossRef]
40. Lee, Y.; Hwang, K. Skin thickness of Korean adults. *Surg. Radiol. Anat.* **2002**, *24*, 183–189. [CrossRef]
41. Dos Santos, D.M.; Leite, I.S.; Bukzem, A.d.L.; de Oliveira Santos, R.P.; Frollini, E.; Inada, N.M.; Campana-Filho, S.P. Nanostructured electrospun nonwovens of poly(ε-caprolactone)/quaternized chitosan for potential biomedical applications. *Carbohydr. Polym.* **2018**, *186*, 110–121. [CrossRef]
42. Rahmani, H.; Najafi, S.H.M.; Ashori, A.; Fashapoyeh, M.A.; Mohseni, F.A.; Torkaman, S. Preparation of chitosan-based composites with urethane cross linkage and evaluation of their properties for using as wound healing dressing. *Carbohydr. Polym.* **2019**, *230*, 115606. [CrossRef]
43. Fougeron, N.; Connesson, N.; Chagnon, G.; Alonso, T.; Pasquinet, L.; Bahuon, M.; Guillen, E.; Perrier, A.; Payan, Y. New pressure ulcers dressings to alleviate human soft tissues: A finite element study. *J. Tissue Viability* **2022**, *31*, 506–513. [CrossRef]
44. Geneviro, G.M.; Gomes Neto, R.J.; Paulo, L.d.A.; Lopes, P.S.; de Moraes, M.A.; Beppu, M.M. Glucomannan asymmetric membranes for wound dressing. *J. Mater. Res.* **2019**, *34*, 481–489. [CrossRef]
45. Kimura, V.T.; Miyasato, C.S.; Genesi, B.P.; Lopes, P.S.; Yoshida, C.M.P.; da Silva, C.F. The effect of andiroba oil and chitosan concentration on the physical properties of chitosan emulsion film. *Polímeros* **2016**, *26*, 168–175. [CrossRef]
46. Pilehvar-Soltanahmadi, Y.; Dadashpour, M.; Mohajeri, A.; Fattahi, A.; Sheervalilou, R.; Zarghami, N. An Overview on Application of Natural Substances Incorporated with Electrospun Nanofibrous Scaffolds to Development of Innovative Wound Dressings. *Mini Rev. Med. Chem.* **2018**, *18*, 414–427. [CrossRef] [PubMed]
47. Surendranath, M.; Rajalekshmi, R.; Ramesan, R.M.; Nair, P.; Parameswaran, R. UV-Crosslinked Electrospun Zein/PEO Fibro-porous Membranes for Wound Dressing. *ACS Appl. Bio Mater.* **2022**, *5*, 1538–1551. [CrossRef]

48. Garcia-Orue, I.; Santos-Vizcaino, E.; Etxabide, A.; Uranga, J.; Bayat, A.; Guerrero, P.; Igartua, M.; de la Caba, K.; Hernandez, R.M. Development of Bioinspired Gelatin and Gelatin/Chitosan Bilayer Hydrofilms for Wound Healing. *Pharmaceutics* **2019**, *11*, 314. [[CrossRef](#)]
49. Chu, Y.; Xu, T.; Gao, C.; Liu, X.; Zhang, N.; Feng, X.; Tang, X. Evaluations of physicochemical and biological properties of pullulan-based films incorporated with cinnamon essential oil and Tween 80. *Int. J. Biol. Macromol.* **2019**, *122*, 388–394. [[CrossRef](#)]
50. Dou, B.; Dupont, V.; Williams, P.T.; Chen, H.; Ding, Y. Thermogravimetric kinetics of crude glycerol. *Bioresour. Technol.* **2009**, *100*, 2613–2620. [[CrossRef](#)]
51. Li, K.; Zhu, J.; Guan, G.; Wu, H. Preparation of chitosan-sodium alginate films through layer-by-layer assembly and ferulic acid crosslinking: Film properties, characterization, and formation mechanism. *Int. J. Biol. Macromol.* **2018**, *122*, 485–492. [[CrossRef](#)]
52. Zhang, W.; Shu, C.; Chen, Q.; Cao, J.; Jiang, W. The multi-layer film system improved the release and retention properties of cinnamon essential oil and its application as coating in inhibition to penicillium expansion of apple fruit. *Food Chem.* **2019**, *299*, 125109. [[CrossRef](#)]
53. Poonguzhali, R.; Basha, S.K.; Kumari, V.S. Synthesis and characterization of chitosan-PVP-nanocellulose composites for in-vitro wound dressing application. *Int. J. Biol. Macromol.* **2017**, *105*, 111–120. [[CrossRef](#)]
54. Khalil, M.M.H.; Ismail, E.H.; El-Magdoub, F. Biosynthesis of Au nanoparticles using olive leaf extract. *Arab. J. Chem.* **2012**, *5*, 431–437. [[CrossRef](#)]
55. Erdogan, I.; Demir, M.; Bayraktar, O. Olive leaf extract as a crosslinking agent for the preparation of electrospun zein fibers. *J. Appl. Polym. Sci.* **2015**, *132*. [[CrossRef](#)]
56. Kiti, K.; Suwantong, O. Bilayer wound dressing based on sodium alginate incorporated with curcumin- β -cyclodextrin inclusion complex/chitosan hydrogel. *Int. J. Biol. Macromol.* **2020**, *164*, 4113–4124. [[CrossRef](#)] [[PubMed](#)]
57. Chang, C.; Duan, B.; Cai, J.; Zhang, L. Superabsorbent hydrogels based on cellulose for smart swelling and controllable delivery. *Eur. Polym. J.* **2010**, *46*, 92–100. [[CrossRef](#)]
58. Ren, H.; Gao, Z.; Wu, D.; Jiang, J.; Sun, Y.; Luo, C. Efficient Pb(II) removal using sodium alginate-carboxymethyl cellulose gel beads: Preparation, characterization, and adsorption mechanism. *Carbohydr. Polym.* **2016**, *137*, 402–409. [[CrossRef](#)]
59. Kubovský, I.; Kačíková, D.; Kačík, F. Structural Changes of Oak Wood Main Components Caused by Thermal Modification. *Polymers* **2020**, *12*, 485. [[CrossRef](#)]
60. Kuila, S.B.; Ray, S.K. Separation of benzene–cyclohexane mixtures by filled blend membranes of carboxymethyl cellulose and sodium alginate. *Sep. Purif. Technol.* **2014**, *123*, 45–52. [[CrossRef](#)]
61. Bayraktar, O. Silk fibroin nanofibers loaded with hydroxytyrosol from hydrolysis of oleuropein in olive leaf extract. *Text. Leather Rev.* **2018**, *1*, 90–98. [[CrossRef](#)]
62. Luciano, C.G.; Rodrigues, M.M.; Lourenço, R.V.; Bittante, A.M.Q.B.; Fernandes, A.M.; do Amaral Sobral, P.J. Bi-layer Gelatin Film: Activating Film by Incorporation of “Pitanga” Leaf Hydroethanolic Extract and/or Nisin in the Second Layer. *Food Bioprocess Technol.* **2021**, *14*, 106–119. [[CrossRef](#)]
63. De la Ossa, J.G.; Fusco, A.; Azimi, B.; Esposito Salsano, J.; Digiocomo, M.; Coltelli, M.-B.; De Clerck, K.; Roy, I.; Macchia, M.; Lazzeri, A.; et al. Immunomodulatory Activity of Electrospun Polyhydroxyalkanoate Fiber Scaffolds Incorporating Olive Leaf Extract. *Appl. Sci.* **2021**, *11*, 4006. [[CrossRef](#)]

Disclaimer/Publisher’s Note: The statements, opinions and data contained in all publications are solely those of the individual author(s) and contributor(s) and not of MDPI and/or the editor(s). MDPI and/or the editor(s) disclaim responsibility for any injury to people or property resulting from any ideas, methods, instructions or products referred to in the content.